Published in IET Signal Processing
Received on 7th June 2013
Revised on 17th August 2013
Accepted on 22nd November 2013
doi: 10.1049/iet-spr.2013.0235

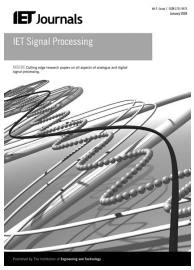

ISSN 1751-9675

# Definition of adaptive detection threshold under employment of the generalised detector in radar sensor systems

*Modar Safir Shbat, Vyacheslav Tuzlukov*

*School of Electronics Engineering, College of IT Engineering, Kyungpook National University, Room 407A, IT Bld# 3, 1370 Sankyuk-dong, Buk-gu, Daegu 702-701, South Korea*
*E-mail: tuzlukov@ee.knu.ac.kr*

**Abstract:** An adaptive detection threshold under employment of the generalised detector (GD) in radar sensor systems is defined. GD is constructed in accordance with the generalised approach to signal processing in noise. To define the GD adaptive threshold based on the observed noise samples, the authors apply an appropriate noise power estimation technique. This study deals with an adaptive GD detection threshold definition as a function of the estimated noise power. Under investigations, they use two noise power estimation procedures. The first is the sliding window technique with the reference cells. The second procedure is based on the adaptive noise power estimation. Comparative analysis of simulation results demonstrates superiority by detection performance in favour of GD implementation in comparison with the well-known constant false alarm rate (CFAR) detectors, namely, cell averaging CFAR and ordered statistics CFAR detectors.

## 1 Introduction

Noise power estimation techniques are widely used in wireless communications, cognitive radio, speech recognition, radar sensors, remote sensing systems and so on. In some wireless communication systems, for example, in worldwide interoperability for microwave access (WiMAX) networks (IEEE 802.16), the noise power estimation procedure is applied to estimate the signal-to-noise ratio (SNR) at the receiver input that is very important parameter for the channel quality control and evaluation of link reliability [1]. As discussed in [2, 3], the proposed noise power estimator in the case of orthogonal frequency-division multiplexing (OFDM) system operates at the receiver front-end based on OFDM principle. The estimator uses the feature of time synchronisation preamble in WiMAX systems [IEEE802.16, 2004]. In OFDM systems, SNR estimation is also used for power control, adaptive coding and modulation, turbo coding etc. Complete knowledge about the noise power at the energy detector input is required, that is, it should be estimated, in the case of energy detector implementation for fast spectrum sensing in cognitive radio systems [4].

The noise power estimation is widely used in radar sensor systems employing the constant false alarm rate (CFAR) detector. In the case of CFAR detector, the noise power is estimated after processing the specified number of reference cells using the sliding window technique. The required detection threshold is defined multiplying the estimated noise power by a scaling factor [5]. The CFAR detectors are differed in processing method of the data in the reference cells. Cell averaging CFAR (CA-CFAR) detector has an optimum performance under the homogenous noise conditions [6]. It estimates the noise power by averaging the data in reference cells of the sliding window. The CA-CFAR detector is the optimum CFAR detector that maximises the probability of detection under the homogeneous noise conditions when the reference cells contain independent and identically distributed (i.i.d.) observations (the CA-CFAR detector uses the maximum likelihood estimate of noise power). The CFAR detector with ordered statistics (OSs-CFAR) is implemented under the non-homogeneous noise and multitarget conditions [7]. The OS-CFAR detector ranks the reference cell data in ascending numerical order with the purpose to form a new sequence where the $k$th-order statistic is selected as the noise power. Many other CFAR detectors are employed under the non-homogeneous noise conditions, for example, the generalised censored mean level (GCML) detector and the adaptive censored greatest-of CFAR (ACGO-CFAR) detector discussed in [8, 9], respectively. The GCML detector discards the data associated with interfering targets before definition of the noise power and detection threshold. Similarly, ACGO-CFAR detector suppresses the clutter edge false alarm determining the average noise power in the leading and lagging windows individually after censoring, and then assigns the maximal averaged noise power as the required estimation.

In [10], a modified OS-CFAR processor called the trimmed mean CFAR (TM-CFAR) detector, which performs a trimmed averaging after ordering, is considered. This paper shows that the TM-CFAR detector may actually perform

somewhat better than the OS-CFAR detector. The TM-CFAR detector combines ordering with arithmetic averaging and is reduced to the CA-CFAR and OS-CFAR schemes at the specific trimming values. Analysis of the generalised order statistic CFAR (GOS-CFAR) detector performance for the correlated Rayleigh target model can be found in [11]. By choice of the GOS-CFAR filter coefficients, the GOS-CFAR can be the OS-CFAR, the TM-CFAR, the censored mean level (CML) or the CA-CFAR detector. For Swerling 2 target model (as in the case of our paper) and under homogeneous noise condition, the CA-CFAR and TM-CFAR detectors have very close detection performance [12].

The adaptive subspace detector (ASD) [13] is a result of adaptation process of the matched subspace detector (MSD) to the unknown noise covariance matrix using the theory of generalised likelihood ratio test (GLRT). The noise power is estimated in order to have a CFAR. The ASD is the adaptive GLRT generalisation of the MSD where the training data are used to estimate the unknown noise covariance matrix and scaled by the same way as the test data. The CFAR ASD is the adaptive GLRT generalisation of the CFAR MSD, but the training data and test data are not uniformly scaled. In the ASD, it is assumed that the training data represent the noise structure accurately, but not the noise level. The CFAR ASD suffers the performance loss under idealised scenario of homogeneity between the training data and test data noise statistics [13].

The generalised detector (GD) is constructed in accordance with the generalised approach to signal processing in noise [14–16]. The GD consists of two channels, namely, the Neyman–Pearson receiver channel and the energy detector channel. The test statistic at the GD output is a result of joint simultaneous operation of the GD Neyman–Pearson receiver and GD energy detector channels [15, Chapter 3]. There are two linear systems at the GD input, namely, the preliminary filter (PF), and the additional filter (AF) as shown in Fig. 1. The PF bandwidth is matched with the bandwidth of the signal to be detected. The PF resonant or central frequency is detuned relatively to the AF resonant or central frequency. This detuning provides the uncorrelated and independent statistics at the PF and AF outputs [17, 18]. Thus, we obtain the signal plus noise at the PF output in the case of a 'yes' signal, and only noise in the case of a 'no' signal, whereas only the noise is obtained at the AF output for both cases, a 'yes' or a 'no' signal. Thus, GD is designed to formulate a decision-making rule (test statistic) for the signal detection rather than a filtering approach which nulls or cancels the interference (signal blocking operation) [15, Chapter 3]. The GD employment in communication systems is discussed in [19–22] and in radar in [23], in particular, in radar sensor systems for short and middle range radar applications such as the closing vehicle detection and blind spot detection in [24–27].

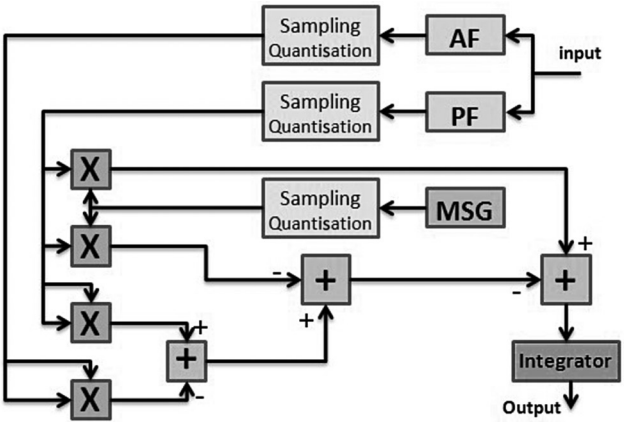


**Fig. 1** *Principal flowchart of GD*

Objective of the present paper is a definition of the GD adaptive detection threshold under employment of appropriate noise power estimation technique. The reference noise at the AF output helps us to perform easily any noise power estimation approach. Thus, we propose to add the noise power estimator module to the main GD structure presented in [14] and [15, Chapter 7, Fig. 7.1]. The GD threshold is defined using the main GD functioning principles [14] and [15, Chapter 3]. To define the instantaneous GD detection threshold, we apply two suitable noise power estimation methods. The first method is the sliding window technique with suitable number of reference cells. The second method is based on the adaptive noise power estimation (ANPE) technique discussed in [28]. We present a comparative analysis between the GD and well investigated types of CFAR detectors, namely, CA-CFAR and OS-CFAR detectors, with the purpose to show GD superiority by detection performance under the homogeneous and non-homogeneous noise conditions in comparison with the CFAR detectors. Discussion of simulation results allows us to make a conclusion that GD demonstrates the better detection performance and robustness against the interfering targets in comparison with the CA-CFAR and OS-CFAR detectors under the same initial conditions.

The rest of this paper is organised as follows. The main GD functioning principles are discussed briefly in Section 2. Section 3 deals with a brief description of the noise power estimation procedures applied to GD. Simulation results are discussed in Section 4. Finally, the conclusion remarks are presented in Section 5.

## 2 GD: main functioning principles

### 2.1 General statement

Let $Y[n]$ be the sample of the input discrete-time stochastic process; $a[n]$ is the sample of the discrete-time target return signal; $w[n]$ is the sample of the discrete-time additive Gaussian noise with zero mean and variance $\sigma^2$; $n = 0, \ldots, N-1$. The simplest signal detection problem can be presented in the following form

$$Y[n] = \begin{cases} a[n] + w[n], & n = 0, \ \ldots, \ N-1 \Rightarrow H_1 \\ w[n], & n = 0, \ \ldots, \ N-1 \Rightarrow H_0 \end{cases} \quad (1)$$

where $N$ is the sample size, $H_1$ is the hypothesis a 'yes' signal and $H_0$ is the alternative hypothesis. If the probability of false alarm $P_{\mathrm{FA}}$ is fixed, there is a problem to define a criterion, for which the probability of detection $P_{\mathrm{D}}$ is maximum for any SNR. In practice, in order to maintain permanently a physical sense of signal detection, the target return signal $a[n]$ should be replaced by its model $a_m[n]$ at the receiver. This model signal, in a general case, is given as $a_m[n] = \mu a[n]$, where $\mu$ is the coefficient of the proportionality, and in particular, in the case of GD, is defined as

$$a_m[n] = a[n] \quad (2)$$




doi: 10.1049/iet-spr.2013.0235

The Equality (2) is the main functioning condition for GD [14], [15, Chapter 3] that is very important for better understanding of GD operation.

The use of GASP in noise assumes some modifications concerning the initial premises of the classical and modern signal detection theories. The signal detection algorithm constructed based on GASP in noise can be presented in the following form [14], [15, Chapter 3] and [16, Chapter 5]

$$\sum_{n=0}^{N-1} 2X[n]a_m[n] - \sum_{n=0}^{N-1} X^2[n] + \sum_{n=0}^{N-1} \eta^2[n] \underset{H_0}{\overset{H_1}{\gtrless}} \mathrm{THR}_{\mathrm{GD}} \quad (3)$$

where $X[n]$ is the sample of the discrete-time observed stochastic process at the PF output, $\eta[n]$ is the sample of discrete-time observed noise at the AF output and $\mathrm{THR}_{\mathrm{GD}}$ is the GD detection threshold. The first term in (3) corresponds to the optimal detector in the Neyman–Pearson criterion sense with twice the gain and is considered as the sufficient statistics of the likelihood mean. The second term in (3) corresponds to the energy detector and is considered as the sufficient statistics of the likelihood variance. The third term in (3) is the power of reference noise formed at the AF output according to the main GD functioning principles. Equation (3) represents the decision-making rule for GD employment in any signal processing system.

### 2.2 GD structure

For better understanding (3), we recall the main GD functioning principles discussed in detail in [14], [15, Chapter 3] and [16, Chapter 5]. The simple GD flowchart is represented in Fig. 1 where model signal generator (MSG) is the local oscillator. For simplicity of analysis, we think that PF and AF have the same amplitude-frequency responses and bandwidths. As we mentioned before, the resonant or central frequency of AF is detuned relative to the PF one on such a value that the signal to be detected cannot pass through the AF. It is well known, if the detuning value between the AF and PF resonant frequencies is more than 4 or 5 times $\Delta f_a$, where $\Delta f_a$ is the bandwidth of the signal to be detected, the processes forming at the AF and PF outputs can be considered as the independent and uncorrelated processes. In practice, the coefficient of correlation between the PF and AF output processes is not more than 0.05 that was confirmed experimentally in [17, 18].

When there is no signal at the GD input, the statistical parameters at the AF and PF outputs are the same, since AF and PF do not change the statistical parameters of input process because they are the linear GD front-end systems. By this reason, AF can be considered as a reference noise source. A detailed discussion of AF and PF can be found in [14], [15, Chapter 3] and [16, Chapter 5]. If the Gaussian noise $w[n]$ with zero mean and power spectral density (PSD) $0.5N_0$ comes in at the AF and PF inputs, the noise forming at the AF and PF outputs is Gaussian too. In a general case, this noise takes the following form

$$\begin{cases} w_{\mathrm{PF}}[n] = \zeta[n] = \sum\limits_{m=-\infty}^{\infty} h_{\mathrm{PF}}[m]w[n-m] \\ w_{\mathrm{AF}}[n] = \eta[n] = \sum\limits_{m=-\infty}^{\infty} h_{\mathrm{AF}}[m]w[n-m] \end{cases} \quad (4)$$

where $h_{\mathrm{PF}}[m]$ and $h_{\mathrm{AF}}[m]$ are the impulse responses of the PF and AF, respectively. The variance of noise forming at the AF and PF outputs is given by [20]

$$\sigma^2 = \frac{N_0\omega_0^2}{8\Delta_F} \quad (5)$$

where in the case if AF (or PF) is the resistance-inductance-capacitance (RLC) oscillatory circuit, the AF (or PF) bandwidth $\Delta_F$ and resonance frequency $\omega_0$ are defined in the following manner $\Delta_F = \pi\beta$, $\omega_0 = (R/\sqrt{\mathrm{LC}})$, where $\beta = (R/2L)$.

The main functioning condition of GD (2) is the equality over the whole range of parameters between the model signal $a_m[n]$ forming at the GD MSG output and the signal to be detected $a[n]$. How we can satisfy this condition in practice is discussed in detail in [14], [15, Chapter 7]. For practical purposes, we may use the GD flowchart presented in Fig. 2, in which the threshold apparatus (THRA) device defines the GD threshold and the signal model generator

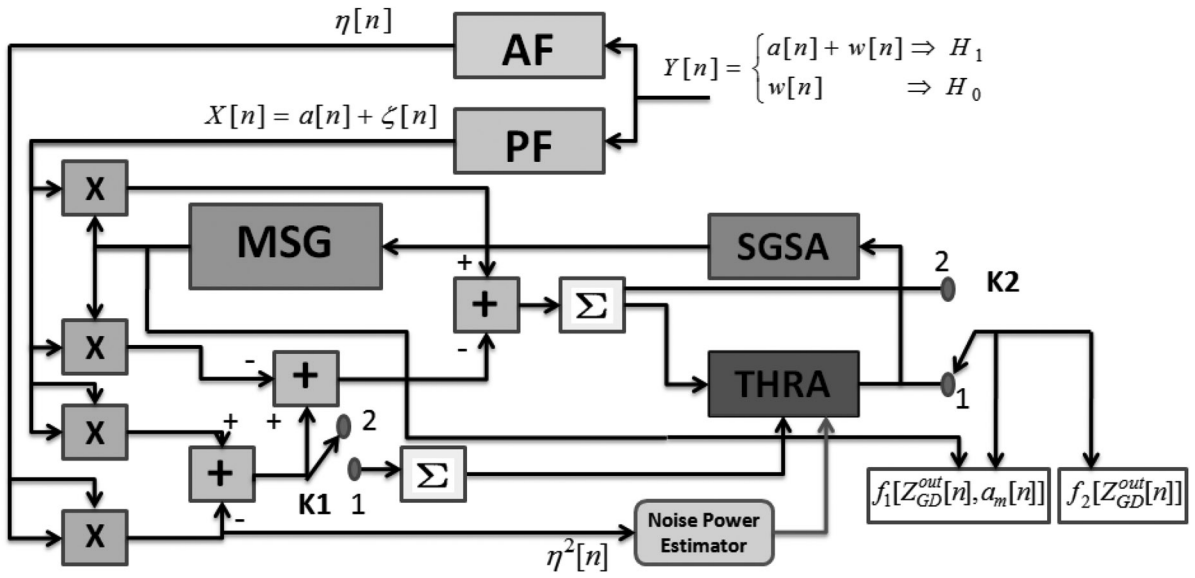


**Fig. 2** *GD structure for practical purposes*

switching apparatus (SGSA) is used to switch on the MSG with the purpose to define the unknown parameters of the target return signal. The switch K1 takes the position '1' to define the GD threshold $\mathrm{THR}_{\mathrm{GD}}$ and takes the position '2' after definition of the GD threshold to carry out a detection of the signal and define its parameters. The switch K2 works to put the THRA in and out of service.

In the case of the signal presence (the hypothesis $H_1$), when $X[n] = a[n] + \zeta[n]$, where $\zeta[n]$ is the sample of the discrete-time observed noise at the PF output, the left side in (3), under the condition given by (2), takes the form

$$\sum_{n=0}^{N-1} a^2[n] + \sum_{n=0}^{N-1} \eta^2[n] - \sum_{n=0}^{N-1} \zeta^2[n]$$

where

$$\sum_{n=0}^{N-1} a^2[n] = E_a$$

is the signal energy, and

$$\sum_{n=0}^{N-1} \eta^2[n] - \sum_{n=0}^{N-1} \zeta^2[n]$$

is the background noise at the GD output. The background noise is a difference between powers of the noise forming at the PF and AF outputs. In the opposite case, if the target return signal is absent (the hypothesis $H_0$), when $X[n] = \zeta[n]$, the left side in (3), under the condition given by (2), is the background noise

$$\sum_{n=0}^{N-1} \eta^2[n] - \sum_{n=0}^{N-1} \zeta^2[n]$$

only that tends to approach zero in the statistical sense.

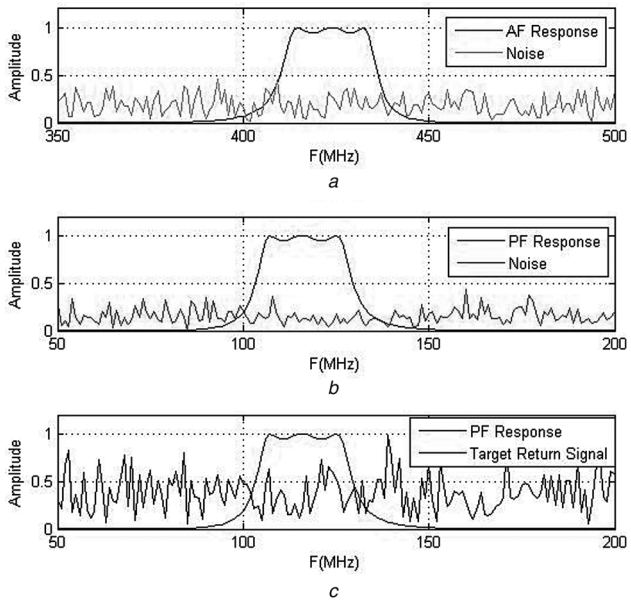


**Fig. 3** *Signals at the PF and AF outputs*

*a* AF response and noise
*b* PF response and noise
*c* PF response and target return signal

Thus, the signal to be detected $a[n]$ plus noise $\zeta[n]$ can be appeared at the PF output and only the reference noise $\eta[n]$ is appeared at the AF output. This statement is illustrated by Fig. 3 where we have only the noise at the AF output regardless of a 'no' or a 'yes' signal at the GD input (Fig. 3*a*), and the noise only or signal plus noise at the PF output, Figs. 3*b* and *c*, respectively. Fig. 3 also shows that PF and AF have the same bandwidth, but the AF central frequency is detuned relative to the PF central frequency.

### 2.3 GD threshold

The Neyman–Pearson criterion is motivated with the purpose to obtain the best detection performance ensuring that the $P_{\mathrm{FA}}$ does not exceed some tolerable value $\alpha$ ($P_{\mathrm{FA}} \le \alpha$). This optimisation problem is solved by the method of Lagrange multipliers, [5, Chapter 6] and [29]. Given a specific model of the probability density function (pdf) at the GD output under hypotheses $H_0$ and $H_1$, the probability of false alarm $P_{\mathrm{FA}}$ and the probability of detection $P_{\mathrm{D}}$ can be defined in the following forms

$$P_{\mathrm{FA}} = \int_{\mathrm{THR}_{\mathrm{GD}}}^{\infty} p(x;\ H_0)\,\mathrm{d}x = \int_{\mathrm{THR}_{\mathrm{GD}}}^{\infty} p_{Z_{\mathrm{GD}}^{H_0}}(x)\,\mathrm{d}x \qquad (6)$$

$$P_{\mathrm{D}} = \int_{\mathrm{THR}_{\mathrm{GD}}}^{\infty} p(x; H_1)\ \mathrm{d}x = \int_{\mathrm{THR}_{\mathrm{GD}}}^{\infty} p_{Z_{\mathrm{GD}}^{H_1}}(x)\ \mathrm{d}x, \qquad (7)$$

where $p_{Z_{\mathrm{GD}}^{H_0}}(x)$ is the background noise pdf at the GD output and $p_{Z_{\mathrm{GD}}^{H_1}}(x)$ is the pdf of decision statistics forming at the GD output under the hypotheses $H_1$. In the case when the noise is the narrow-band process with the Rayleigh amplitude envelope and the phase uniformly distributed within the limits of the interval $[0, 2\pi]$, the pdf $p_{Z_{\mathrm{GD}}^{H_0}}(z)$ at the GD output (the background noise pdf) can be determined in the following form [15, Chapter 3]

$$p_{Z_{\mathrm{GD}}^{H_0}}(z) = \begin{cases} \dfrac{1}{2\sigma^2}\exp\left(-\dfrac{|z|}{2\sigma^2}\right), & z \ge 0 \\ 0, & z < 0 \end{cases} \qquad (8)$$

As we can see from (8), the background noise pdf at the GD output is defined by the exponential-type law when the observation time interval $[0, T]$ is infinitesimal ($T \to 0$). Based on (8), the probability of false alarm $P_{\mathrm{FA}}$ can be presented in the following form

$$P_{\mathrm{FA}}^{\mathrm{GD}} = \int_{\mathrm{THR}_{\mathrm{GD}}}^{\infty} p_{Z_{\mathrm{GD}}^{H_0}}(z)\,\mathrm{d}z = \exp\left(-\frac{\mathrm{THR}_{\mathrm{GD}}}{2\sigma^2}\right) \qquad (9)$$

According to (9), the GD threshold in terms of $P_{\mathrm{FA}}^{\mathrm{GD}}$ can be presented by the following equation

$$\mathrm{THR}_{\mathrm{GD}} = -2\sigma^2 \ln(P_{\mathrm{FA}}^{\mathrm{GD}}) \qquad (10)$$

If the scaling factor $\gamma_{\mathrm{GD}} = -2\ln(P_{\mathrm{FA}}^{\mathrm{GD}})$ is used, the modified GD threshold is given by

$$\mathrm{THR}_{\mathrm{GD}} = \sigma^2 \gamma_{\mathrm{GD}} \qquad (11)$$

Based on the scaling factor, the probability of false alarm $P_{\mathrm{FA}}^{\mathrm{GD}}$




doi: 10.1049/iet-spr.2013.0235

can be presented in the following form

$$P_{\mathrm{FA}}^{\mathrm{GD}} = \exp\left(-0.5\gamma_{\mathrm{GD}}\right) \tag{12}$$

The last equation allows us to determine the probability of false alarm $P_{\mathrm{FA}}^{\mathrm{GD}}$ for a given scaling factor $\gamma_{\mathrm{GD}}$ or, more likely, to determine the required scaling factor $\gamma_{\mathrm{GD}}$ for the desired probability of false alarm $P_{\mathrm{FA}}^{\mathrm{GD}}$.

### 2.4 GD probability of detection

Based on (8), the pdf of the decision statistics at the GD output under the hypothesis $H_1$ can be presented in the following form

$$p_{Z_{\mathrm{GD}}^{H_1}}(z) = \frac{1}{2(\sigma_{\mathrm{s}}^2 + \sigma^2)} \exp\left(-\frac{z}{2(\sigma_{\mathrm{s}}^2 + \sigma^2)}\right) \tag{13}$$

where $\sigma_{\mathrm{s}}^2$ is the variance of the fluctuating target return signal modelled as Swerling 2 model. The probability of detection $P_{\mathrm{D}}^{\mathrm{GD}}$ can be determined as

$$\begin{aligned} P_{\mathrm{D}}^{\mathrm{GD}} &= \int_{\mathrm{THR}_{\mathrm{GD}}}^{\infty} p_{Z_g^{H_1}}(z)\,\mathrm{d}z \\ &= \int_{\mathrm{THR}_{\mathrm{GD}}}^{\infty} \frac{1}{2(\sigma_{\mathrm{s}}^2 + \sigma^2)} \exp\left(-\frac{z}{2(\sigma_{\mathrm{s}}^2 + \sigma^2)}\right)\mathrm{d}z \\ &= \int_{\mathrm{THR}_{\mathrm{GD}}}^{\infty} \frac{1}{2\sigma^2(1+\mathrm{SNR})} \exp\left(-\frac{z}{2\sigma^2(1+\mathrm{SNR})}\right)\mathrm{d}z \end{aligned} \tag{14}$$

where $\mathrm{SNR} = \sigma_{\mathrm{s}}^2/\sigma^2$ is the SNR at the GD input. Taking into consideration (10) and based on (14) we can define the probability of detection $P_{\mathrm{D}}^{\mathrm{GD}}$ in the following form

$$P_{\mathrm{D}}^{\mathrm{GD}} = \exp\left(-\frac{\mathrm{THR}_{\mathrm{GD}}}{2\sigma^2(1+\mathrm{SNR})}\right) = \exp\left(\frac{\ln(P_{\mathrm{FA}}^{\mathrm{GD}})}{1+\mathrm{SNR}}\right) \tag{15}$$

## 3 Noise power estimation

If the noise variance $\sigma^2$ at the AF and PF outputs is assumed to be constant, then the fixed GD threshold can satisfy (10). However, owing to non-stationary scenario in practice, this condition is not satisfied. Thus, in order to maintain the constant probability of false alarm $P_{\mathrm{FA}}$ required to achieve the acceptable performance stability, the GD threshold should be adaptively updated or changed based on the noise variance at the AF and PF outputs (the noise power at PF and AF outputs is the same). Thus, there is a need to apply some noise power estimation technique in order to define the adaptive GD threshold. Owing to the fact that the expected return signals from interfering targets are located within the limits of PF bandwidth, the noise power estimation is not affected by these interfering signals. In the case, when the interference is included into the AF bandwidth from jammer or any other sources, the noise power estimation procedure will be affected.

Two different noise power estimation procedures are considered with the purpose to be used by GD. The first procedure is the sliding window technique used to estimate the noise power by processing a group of reference cells and the second one is called the ANPE.

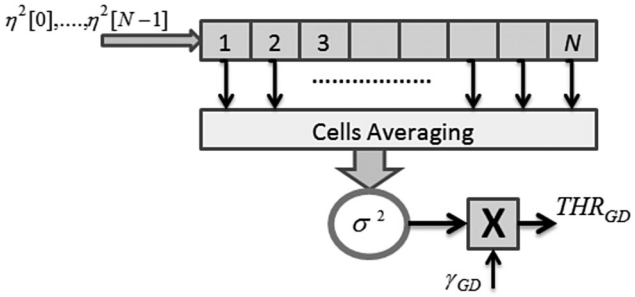


**Fig. 4** *Cell averaging sliding window technique*

### 3.1 Noise power estimation based on sliding window technique

The noise power estimation approach based on sliding window technique is simple and effective. The noise power estimator contains $N$ reference cells. The available data (the squared noise samples at the GD AF output) in the reference cells are processed by a special algorithm to define the estimated noise power. By this approach, the estimated noise power is obtained by processing the reference cells (the cell averaging technique) [5, 6]. This technique is widely adopted by the CA-CFAR detectors [5, Chapter 7], [30–33] (Fig. 4). There is a need to mention that this technique works under assumption that noise samples in the reference cells of the sliding window are i.i.d. For this technique, the estimated noise power can be obtained by processing the squared noise sample $\eta[n]$, $n = 0, \ldots, N-1$ forming at the AF output in the following form

$$\hat{\sigma}^2 = \frac{1}{N}\sum_{n=0}^{N-1} \eta^2[n] \tag{16}$$

Taking into consideration (16), the GD detection threshold can be easily defined as

$$\mathrm{THR}_{\mathrm{GD}} = -2\hat{\sigma}^2 \ln(P_{\mathrm{FA}}) \tag{17}$$

The number of the reference cells $N$ in the sliding window determines the noise power estimation accuracy. Small value of $N$ leads to the poor detection performance and high noise power estimation error. As the number of reference cells $N$ becomes large ($N \to \infty$), the noise power estimation should be converged to the true value [5, Chapter 7]. In practice, $N$ is chosen based on tradeoff between the CFAR losses, complexity and required accuracy [34].

The definition of the average probability of detection $P_{\mathrm{D_{av}}}^{\mathrm{GD}}$ helps us to find a relationship between the GD detection performance and the number of reference cells in the sliding window $N$. According to [5, Chapter 7], the average probability of detection $P_{\mathrm{D_{av}}}^{\mathrm{GD}}$ is defined using the following form

$$P_{\mathrm{D_{av}}}^{\mathrm{GD}} = \int_{-\infty}^{\infty} P_{\mathrm{D}}^{\mathrm{GD}} p(\mathrm{THR}_{\mathrm{GD}})\,\mathrm{d}(\mathrm{THR}_{\mathrm{GD}}) \tag{18}$$

where $p(\mathrm{THR}_{\mathrm{GD}})$ is the GD threshold pdf that can be determined in the following form based on the procedure

discussed in [5, Chapter 6]

$$p(\mathrm{THR}_{\mathrm{GD}}) = \left(\frac{N}{\gamma_{\mathrm{GD}}\sigma^2}\right)^N \frac{\mathrm{THR}_{\mathrm{GD}}^{N-1}}{(N-1)!} \exp\left(-N\frac{\mathrm{THR}_{\mathrm{GD}}}{\gamma_{\mathrm{GD}}\sigma^2}\right) \quad (19)$$

Based on (18) and (19), the average probability of detection $P_{\mathrm{D_{av}}}^{\mathrm{GD}}$ is determined as (see (20))

Using the tabulated integral [35]

$$\int_0^\infty x^b \exp(-ax) = \frac{b!}{a^{b+1}}, \quad a > 0, \quad b = 0,\ 1,\ 2,\ \ldots \quad (21)$$

we can find that the average probability of detection $P_{\mathrm{D_{av}}}^{\mathrm{GD}}$ is determined in the following form

$$P_{\mathrm{D_{av}}}^{\mathrm{GD}} = \left(1 + \frac{\gamma_{\mathrm{GD}}}{2N(1+\mathrm{SNR})}\right)^{-N} \quad (22)$$

In general, the detector will be considered to be CFAR if the expected or averaged value of the probability of false alarm does not depend on the actual value of noise power. In the case of GD, the expected value of $P_{\mathrm{FA}}^{\mathrm{GD}}$ is defined as (see (23))

Taking into consideration (21), solution of (23) has the following form

$$P_{\mathrm{FA_{av}}}^{\mathrm{GD}} = \left(1 + \frac{\gamma_{\mathrm{GD}}}{2N}\right)^{-N} \quad (24)$$

From (24), we can note that the expected average probability of false alarm $P_{\mathrm{FA_{av}}}^{\mathrm{GD}}$ of the GD does not depend on the actual noise power $\sigma^2$. Thus, the GD exhibits the CFAR behaviour. Actually, the observed probability of false alarm $P_{\mathrm{FA_{ob}}}^{\mathrm{GD}}$ will vary from the desired value. The degree of this variation can be defined numerically. Let $P_{\mathrm{FA_{des}}}^{\mathrm{GD}}$ be the desired probability of false alarm of the GD when the estimated noise power is equal to $\widehat{\sigma}^2$. The GD threshold in this case is given as $\mathrm{THR}_{\mathrm{GD}} = -2\widehat{\sigma}^2 \ln(P_{\mathrm{FA_{des}}}^{\mathrm{GD}})$. Taking into consideration (9), we can determine the observed probability of false alarm of the GD $P_{\mathrm{FA_{ob}}}^{\mathrm{GD}}$ using the following form

$$P_{\mathrm{FA_{ob}}}^{\mathrm{GD}} = \exp\left\{\frac{2\widehat{\sigma}^2 \ln(P_{\mathrm{FA_{des}}}^{\mathrm{GD}})}{2\sigma^2}\right\} = \exp\left\{\ln\left\{\left[P_{\mathrm{FA_{des}}}^{\mathrm{GD}}\right]^{(\widehat{\sigma}^2/\sigma^2)}\right\}\right\} = \left[P_{\mathrm{FA_{des}}}^{\mathrm{GD}}\right]^{(\widehat{\sigma}^2/\sigma^2)} \quad (25)$$

We can conclude that if the real and estimated noise powers are the same, then the desired and observed probabilities of false alarm are the same too.

To quantify the CFAR loss in the GD case, we should combine (22) and (24) to eliminate the scaling factor $\gamma_{\mathrm{GD}}$ and then solve this combination with respect to SNR. We obtain the SNR needed to achieve the specified average probability of detection $P_{\mathrm{D_{av}}}^{\mathrm{GD}}$ and average probability of false alarm $P_{\mathrm{FA_{av}}}^{\mathrm{GD}}$ when the finite number of reference cells $N$ is used

$$\mathrm{SNR}_N = \frac{\left[P_{\mathrm{D_{av}}}^{\mathrm{GD}}/P_{\mathrm{FA_{av}}}^{\mathrm{GD}}\right]^{1/N} - 1}{1 - (P_{\mathrm{D_{av}}}^{\mathrm{GD}})^{1/N}} \quad (26)$$

Now, taking the logarithm of the average probability of false alarm $P_{\mathrm{FA_{av}}}^{\mathrm{GD}}$ given by (24), and applying the Taylor series expansion we obtain

$$\ln(P_{\mathrm{FA_{av}}}^{\mathrm{GD}}) = \ln\left\{\left(1 + \frac{\gamma_{\mathrm{GD}}}{2N}\right)^{-N}\right\} = -N\ln\left(1 + \frac{\gamma_{\mathrm{GD}}}{2N}\right) = -N\left[\frac{\gamma_{\mathrm{GD}}}{2N} - \frac{1}{2}\left(\frac{\gamma_{\mathrm{GD}}}{2N}\right)^2 + \cdots\right] \quad (27)$$

As the number of reference cells tends to approach infinity ($N \to \infty$), we can define the limit of (27)

$$\lim_{N\to\infty} \ln(P_{\mathrm{FA_{av}}}^{\mathrm{GD}}) = -N\left(\frac{\gamma_{\mathrm{GD}}}{2N}\right) \Rightarrow \lim_{N\to\infty} P_{\mathrm{FA_{av}}}^{\mathrm{GD}} = \exp\left(-\frac{\gamma_{\mathrm{GD}}}{2}\right) \quad (28)$$

Applying the same procedure, we can define the limit of the average probability of detection $P_{\mathrm{D_{av}}}^{\mathrm{GD}}$ at $N \to \infty$ as

$$\lim_{N\to\infty} P_{\mathrm{D_{av}}}^{\mathrm{GD}} = \exp\left(-\frac{\gamma_{\mathrm{GD}}}{2(1+\mathrm{SNR})}\right) \quad (29)$$

Based on (28) and (29), we can determine the SNR required to achieve the desired probability of detection $P_{\mathrm{D_{des}}}^{\mathrm{GD}}$ and probability of false alarm $P_{\mathrm{FA_{des}}}^{\mathrm{GD}}$ at $N \to \infty$ using the following form

$$\mathrm{SNR}_\infty = \frac{\ln(P_{\mathrm{FA_{av}}}^{\mathrm{GD}}/P_{\mathrm{D_{av}}}^{\mathrm{GD}})}{\ln(P_{\mathrm{D_{av}}}^{\mathrm{GD}})} \quad (30)$$

The CFAR loss in the GD case can be represented using the following form

$$L_{\mathrm{CFAR}}^{\mathrm{GD}} = \frac{\mathrm{SNR}_N}{\mathrm{SNR}_\infty} = \frac{\ln(P_{\mathrm{D_{av}}}^{\mathrm{GD}})}{\ln(P_{\mathrm{FA_{av}}}^{\mathrm{GD}}/P_{\mathrm{D_{av}}}^{\mathrm{GD}})} \times \frac{(P_{\mathrm{D_{av}}}^{\mathrm{GD}}/P_{\mathrm{FA_{av}}}^{\mathrm{GD}})^{1/N} - 1}{1 - (P_{\mathrm{D_{av}}}^{\mathrm{GD}})^{1/N}} \quad (31)$$

$$P_{\mathrm{D_{av}}}^{\mathrm{GD}} = \int_{-\infty}^{\infty} \left(\frac{N}{\gamma_{\mathrm{GD}}\sigma^2}\right)^N \frac{\mathrm{THR}_{\mathrm{GD}}^{N-1}}{(N-1)!} \exp\left(-\frac{\mathrm{THR}_{\mathrm{GD}}}{2\gamma_{\mathrm{GD}}\sigma^2}\frac{2N(1+\mathrm{SNR})+\gamma_{\mathrm{GD}}}{1+\mathrm{SNR}}\right) \mathrm{d}(\mathrm{THR}_{\mathrm{GD}}) \quad (20)$$

$$P_{\mathrm{FA_{av}}}^{\mathrm{GD}} = \int_{-\infty}^{+\infty} \exp\left(-\frac{\mathrm{THR}_{\mathrm{GD}}}{2\sigma^2}\right) p(\mathrm{THR}_{\mathrm{GD}})\,\mathrm{d}(\mathrm{THR}_{\mathrm{GD}}) = \int_{-\infty}^{+\infty} \left(\frac{N}{\gamma_{\mathrm{GD}}\sigma^2}\right)^N \frac{\mathrm{THR}_{\mathrm{GD}}^{N-1}}{(N-1)!} \exp\left(-\frac{\mathrm{THR}_{\mathrm{GD}}(2N+\gamma_{\mathrm{GD}})}{2\gamma_{\mathrm{GD}}\sigma^2}\right) \mathrm{d}(\mathrm{THR}_{\mathrm{GD}}) \quad (23)$$




doi: 10.1049/iet-spr.2013.0235

### 3.2 Adaptive noise power estimation

The ANPE technique is used usually under explicit detection of time segments that contain only the noise. Thus, it is suitable to be applied for the GD because the reference noise sample $\eta[n]$, $n=0, \ldots, N-1$ is formed at the AF output independently of the noise sample $\zeta[n]$, $n=0, \ldots, N-1$ forming at the PF output. Using ANPE technique [28], the noise amplitude envelope is defined based on assumption that it is varied slowly with respect to frequency and subjected to the Rayleigh pdf. Under this condition, the noise power estimator defines the noise amplitude peaks and classifies them independently in the frequency domain. The overshoots of observed noise amplitude peaks are excluded and the average noise power is estimated based on the remaining noise amplitude peaks.

In the additive white Gaussian noise (AWGN) case, the noise PSD is constant over the whole frequency band. After AWGN filtering by the AF, the noise PSD will be not stationary. Thus, the filtered noise at the AF output may be called as the coloured noise. The coloured noise average power can be estimated by averaging the observed noise amplitude peaks. We assume that the noise at the AF output is coloured within the limits of the AF bandwidth and obeys the Rayleigh distribution. The Rayleigh random variable $x$ is subjected to the following pdf [36, Chapter 2]

$$p(x) = \frac{x}{\sigma_n^2} \exp\left(-\frac{x^2}{2\sigma^2}\right), \quad 0 \le x \le \infty \tag{32}$$

The cumulative distribution function of the Rayleigh random variable $x$ is given by [34, Chapter 2]

$$F(x) = 1 - \exp\left(-\frac{x^2}{2\sigma^2}\right) \tag{33}$$

The $j$th order percentile is a comparison score below that a certain per cent of observations fall or may be found. This score can be presented in the following form [28]

$$x_j = F^{-1}(j) = \beta\sqrt{-2\lg(1-j)}, \quad 0 < j < 1 \tag{34}$$

where $\beta$ corresponds to the mode of the Rayleigh distribution. The variance of the Rayleigh distributed random variable $x$ is determined in the following form [28]

$$\mathrm{Var}(x) = \sigma^2 = \frac{4-\pi}{2}\beta \tag{35}$$

Based on this noise power estimation technique, the noise samples forming at the AF output are analysed in the frequency domain and the discrete Fourier transform is applied. In this case, for each frequency bin $k$, the AF output noise distribution in the frequency domain can be presented as the Rayleigh pdf with the mode $\beta(k)$ used to define a reference noise amplitude envelope $L_\sigma$. The desired noise amplitude envelope $L_n$ can be estimated by simple way using (34) and we obtain the following result

$$L_n = L_\sigma\sqrt{-2\lg(1-j)} \tag{36}$$

The mean of the Rayleigh random variable $x$ is given by

$$E[x] = \beta(k)\sqrt{\pi/2} \tag{37}$$

As follows from (28), the frequency dependent mode $\beta(k)$ can be presented in the following form

$$\beta(k) = \frac{E[x]}{\sqrt{\pi/2}} \tag{38}$$

The frequency dependent mode $\beta(k)$ can be obtained if the mean of the noise components, which is also frequency dependent, is estimated. More details about ANPE technique can be found in [28].

## 4 Simulation results

The simulation results for ANPE technique are presented in Fig. 5, when the sampling frequency is 10 kHz and $j=0.8$ that means only 20% of the noise can be misclassified according to Rayleigh distribution. Owing to choice of PF and AF impulse responses and relation between their central or resonant frequencies, there are no interfering signals at the AF output, and, as it was proven by simulation that is not included in the paper, the variations in the sampling frequency and noise percentile $j$ of the Rayleigh distribution are not important for the noise power estimation and, as a consequence, for definition of the GD threshold.

For the CA-CFAR detector, we can define the probability of detection $P_{\mathrm{D}}^{\mathrm{CA-CFAR}}$ using the pdf of data samples in the reference cells. The pdf of data samples is given by

$$p_x(x) = \frac{1}{\sigma^2}\exp\left(-\frac{x}{\sigma^2}\right), \quad x \ge 0 \tag{39}$$

By the same way, the probability of detection $P_{\mathrm{D}}^{\mathrm{CA\text{-}CFAR}}$ is obtained as

$$\begin{aligned} P_{\mathrm{D}}^{\mathrm{CA\text{-}CFAR}} &= \int_{\mathrm{THR_{CA}}}^{\infty} \frac{1}{\sigma_{\mathrm{s}}^2+\sigma^2}\exp\left(-\frac{x}{\sigma_{\mathrm{s}}^2+\sigma^2}\right)\mathrm{d}x \\ &= \int_{\mathrm{THR_{CA}}}^{\infty} \frac{1}{\sigma^2(1+\mathrm{SNR})}\exp\left(-\frac{x}{\sigma^2(1+\mathrm{SNR})}\right)\mathrm{d}x \\ &= \exp\left(-\frac{\mathrm{THR_{CA\text{-}CFAR}}}{\sigma^2(1+\mathrm{SNR})}\right) = \exp\left(-\frac{\gamma_{\mathrm{CA\text{-}CFAR}}}{1+\mathrm{SNR}}\right) \end{aligned} \tag{40}$$

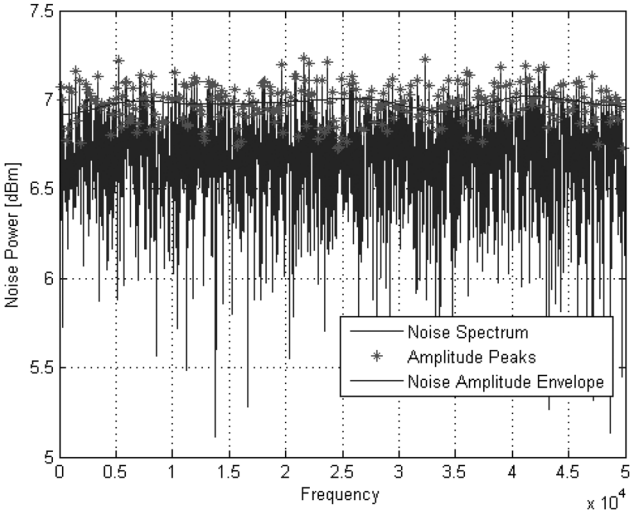


**Fig. 5** *Estimated noise level using ANPE*

where $\mathrm{THR}_{\text{CA-CFAR}} = \sigma^2 \gamma_{\text{CA-CFAR}}$ is the CA-CFAR detector threshold, and $\gamma_{\text{CA-CFAR}}$ is the scaling factor given by

$$\gamma_{\text{CA-CFAR}} = N[(P_{\text{FA}}^{\text{CA-CFAR}})^{-1/N} - 1] \tag{41}$$

The definition of the average probability of detection $P_{\text{D}_{\text{av}}}^{\text{CA-CFAR}}$ of the CA-CFAR detector can be derived by analogous way as in the case of GD [6]

$$P_{\text{D}_{\text{av}}}^{\text{CA-CFAR}} = \left(1 + \frac{\gamma_{\text{CA-CFAR}}}{N(1+\text{SNR})}\right)^{-N} \tag{42}$$

The simulated probability of detection $P_{\text{D}}$ is defined as the ratio between the number $L$ of overshoots with respect to the detection threshold to the total number of observations $M$ [37]

$$P_{\text{D}} = \frac{L}{M} \tag{43}$$

We compare the GD, CA-CFAR detector and OS-CFAR detector by detection performance under the same initial conditions: the probability of false alarm $P_{\text{FA}}$ is equal to $10^{-3}$ and $10^{-4}$; the number of reference cells used for noise power estimation by these detectors is also the same, $N = 20$; and the number of observations is $M = 1000$. The radar sensor target and the interfering target fluctuation models are described by the Swerling 2 model. We define the interfering targets in the following form. When there is one target in the test cell, and one or more targets located among the reference cells in the sliding window assuming that the power of those targets exceeds the power of the noise samples in the surrounding reference cells, the presence of those targets will raise the estimate noise power value and, as a consequence, the detection threshold. We called these targets the interfering targets [5, Chapter 7].

The theoretical probability of detection $P_{\text{D}}$ and the average probability of detection for both detectors $P_{\text{D}_{\text{av}}}^{\text{CA-CFAR}}$ and $P_{\text{D}_{\text{av}}}^{\text{GD}}$ as a function of SNR are presented in Fig. 6 based on (15), (22), (31) and (32) assuming that the GD noise power estimation is based on the sliding window technique (Section 3.1) and the probability of false alarm $P_{\text{FA}}$ is equal to $10^{-3}$ and $10^{-4}$ with the number of reference cells $N = 20$. The GD demonstrates the better detection performance in comparison with the CA-CFAR detector. For example, at the probability of false alarm $P_{\text{FA}}$ equal to $10^{-4}$ when the probability of detection $P_{\text{D}}$ is equal to 0.6, the SNR gain in favour of GD is approximately 1.7 dB.

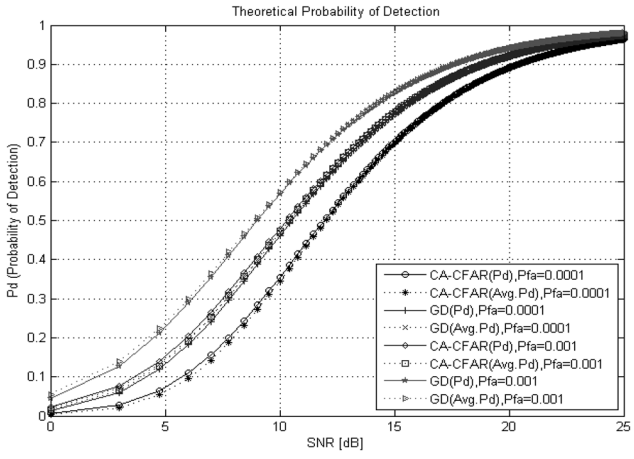


**Fig. 6** *Comparison between the theoretical CA-CFAR and GD detection performances*

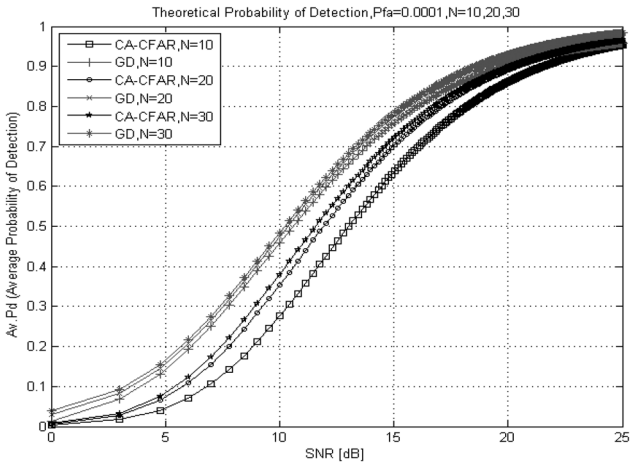


**Fig. 7** *Effect of the number of reference cells N on the CA-CFAR and GD detection performance: the same noise power estimation procedure is used for both detectors*

Detection performances of GD and CA-CFAR detector as a function of SNR are illustrated in Fig. 7 at $N = 10, 20, 30$. As we can see from Fig. 7, the number of reference cells $N$ has a great impact on the CA-CFAR detector performance in comparison with the GD one. As was shown in [5, Chapter 7], the condition $N < 10$ is not acceptable in practice owing to high CFAR detection losses.

The receiver operating characteristic (ROC) curves of GD and CA-CFAR detector are presented in Fig. 8 at $\text{SNR} = 10$ and 15 dB. At the same probability of false alarm $P_{\text{FA}}$, the GD demonstrates the better probability of detection $P_{\text{D}}$ in comparison with the CA-CFAR detector. For example, at $\text{SNR} = 15$ dB and for $P_{\text{FA}} = 10^{-5}$, the probability of detection $P_{\text{D}}$ in the case of CA-CFAR is 0.62, whereas in the case of GD, the probability of detection $P_{\text{D}}$ is equal to 0.72.

In the case of GD, the observed or simulated probability of false alarm $P_{\text{FA}_{\text{ob}}}^{\text{GD}}$ is determined by calculation of the number $L$ in (43) when the target return signal power is equal to zero. Table 1 compares the desired probability of false alarm $P_{\text{FA}_{\text{des}}}^{\text{GD}}$

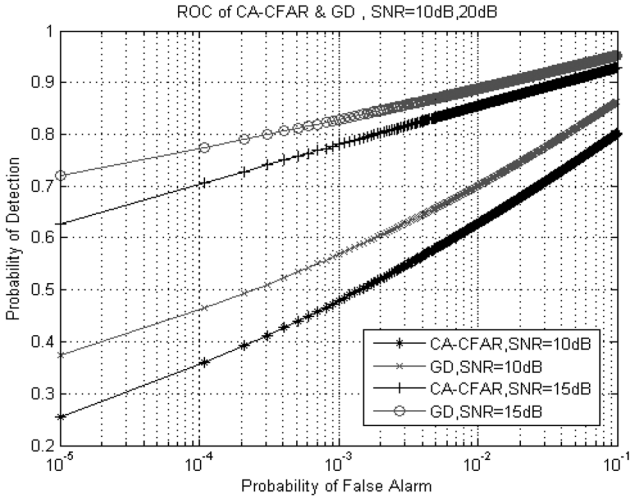


**Fig. 8** *ROC of GD and CA-CFAR detector*




doi: 10.1049/iet-spr.2013.0235

**Table 1** GD desired and observed probabilities of false alarm

| $P_{FA_{des}}^{GD}$ | Number of false alarms | | $P_{FA_{des}}^{GD} \times M$ |
|---|---|---|---|
| | $N = 20$ | $N = 40$ | |
| $10^{-4}$ | 0 | 0 | 0.1 |
| $10^{-3}$ | 3 | 2 | 1 |
| $10^{-2.5}$ | 6 | 5 | 3.2 |
| $10^{-2}$ | 13 | 11 | 10 |
| $10^{-1.5}$ | 34 | 32 | 31.6 |
| $10^{-1}$ | 102 | 96 | 100 |
| $10^{-0.5}$ | 319 | 313 | 316.2 |

and the simulated probability of false alarm $P_{FA_{ob}}^{GD}$ for GD at $N = 20$; 40 and $M = 1000$.

As we can see from Table 1, there is a small difference between the desired probability of false alarm $P_{FA_{des}}^{GD}$ and the observed or simulated probability of false alarm $P_{FA_{ob}}^{GD}$. Thus, the theoretical number of false alarms is not perfectly identical with the simulated one. By this reason, we can believe that the GD has the asymptotic CFAR property.

The CFAR losses for CA-CFAR detector and GD are presented in Fig. 9 as a function of the average probability of detection $P_{D_{av}}$ at $N = 20$; 30 when the average probability of false alarm $P_{FA_{av}}$ is equal to $10^{-3}$ and $10^{-4}$. As follows from Fig. 9, the CFAR loss increases with increasing in the average probability of detection $P_{D_{av}}$ if the average probability of false alarm $P_{FA_{av}}$ and the number of reference cells $N$ are fixed. For both detectors, the CFAR loss is increased at the low average probability of false alarm $P_{FA_{av}}$ and decreased with increasing in the number of reference cells $N$. The GD CFAR loss is less in comparison with CA-CFAR detector one. For example, when the average probability of detection $P_{D_{av}}$ is equal to 0.6 and the average probability of false alarm $P_{FA_{av}}$ is equal to $10^{-3}$ at $N = 30$, the CFAR loss is equal to 1.5 dB in the case of CA-CFAR detector, whereas the CFAR loss is 1 dB in the case of GD.

Fig. 10 demonstrates the simulation results of the detection performances for the CA-CFAR detector and GD when the two suggested noise power estimation procedures are applied to GD, namely, the sliding window technique (Section 3.1) at $N = 20$ and ANPE technique (Section 3.2) at $j = 0.8$ and the sampling frequency is equal to 10 kHz

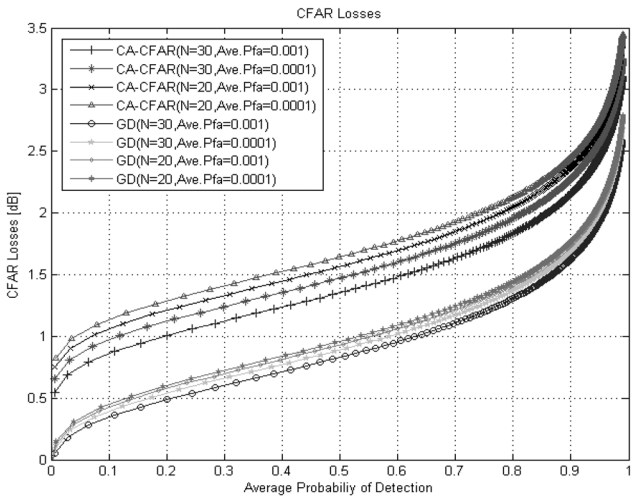


**Fig. 9** *Comparison of CFAR losses between the GD and CA-CFAR detector*

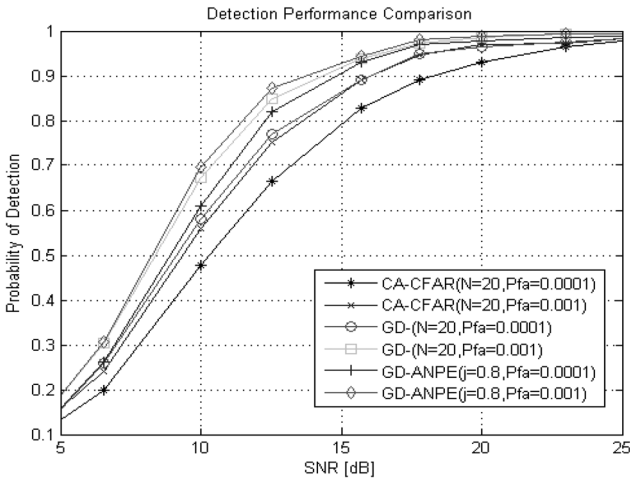


**Fig. 10** *CA-CFAR and GD detection performance*

GD employs two noise power estimation procedures: the sliding window and ANPE

when the probability of false alarm $P_{FA}$ is $10^{-3}$ and $10^{-4}$. The GD SNR gain is 2 dB employing the sliding window technique and 2.5 dB using the ANPE procedure, respectively, in comparison with the CA-CFAR detector at the probability of detection $P_D$ equal to 0.6 and the probability of false alarm $P_{FA}$ equal to $10^{-4}$. As we can see from Fig. 10, at SNR $\leq$ 7 dB, the GD demonstrates almost the same detection performance for both noise power estimation procedures. If SNR > 7 dB, the ANPE technique leads us to the better detection performance in comparison with the sliding window one. Thus, in the case of high SNR, the ANPE technique is preferable, but the sliding window technique is simple under implementation in practice and preferable for the multitarget detection scenario.

Fig. 11 presents a comparison between the detection performances of the CA-CFAR detector, OS-CFAR detector and GD using the sliding window technique at $N = 20$ and $P_{FA} = 10^{-4}$ for all detectors under the three cases: no interference, one interfering target and two interfering targets. We assume that the interfering target signal power

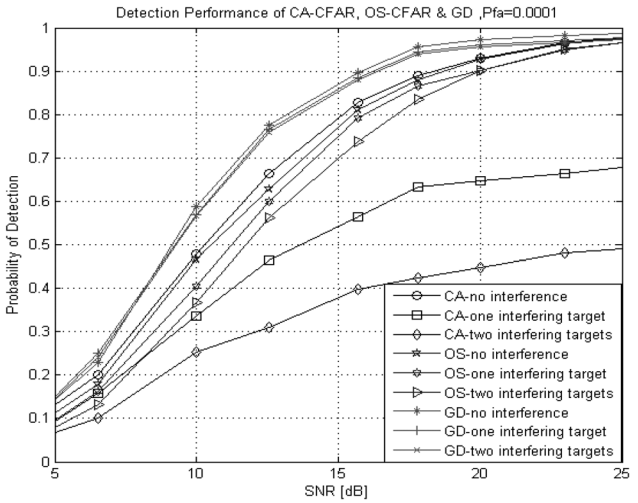


**Fig. 11** *Comparison of the CA-CFAR detector, OS-CFAR detector and GD detection performance for three cases: no interference, one interfering target and two interfering targets*

is equal to the target return signal power that means, consequently, that the interference-to-noise ratio is equal to SNR. In the case of GD, the frequency content of interfering signals is within the limits of PF bandwidth. Obtained results demonstrate a superiority of GD over the CA-CFAR and OS-CFAR detectors under all the considered cases. For example, in the case of one interfering target when the probability of detection $P_D$ is 0.6, the SNR gain in favour of GD is approximately 6.3 dB comparing with the CA-CFAR detector and 2 dB in comparison with the OS-CFAR detector. In the case of two interfering targets, the GD achieves the SNR gain equal to 2.8 dB in comparison with the OS-CFAR detector while the CA-CFAR detector performance degradation is severe. The GD presents a high robustness against the interfering targets, because such interference does not affect on the GD background noise power estimation and, consequently, on the definition of the adaptive GD detection threshold since the reference noise at the AF output is used for the noise power estimation. The case, when the frequency content of interfering signals is outside the limits of GD PF bandwidth and is within the limits of GD AF bandwidth, is outside the scope of the present paper. This case is a further research of GD in the presence of interfering targets.

## 5 Conclusions

The detection threshold should be determined in accordance with the observed noise power under the condition when the noise power $\sigma^2$ is non-stationary. The signal detection with adaptive threshold updated or varied continuously based on the noise variance is very essential in order to achieve the constant probability of false alarm $P_{FA}$ and improve the detection performance.

Based on the simulation results, we see that the GD demonstrates the better detection performance at the same initial conditions and guarantees a superiority in the probability of detection $P_D$ in comparison with the CA-CFAR and OS-CFAR detectors without interfering targets (homogeneous noise condition) and with interfering targets (non-homogeneous noise condition).

The simulation results demonstrate that using the sliding window technique and ANPE procedure for noise power estimation, the GD has the same detection performance if $SNR \leq 7$ dB. When $SNR > 7$ dB, the GD employing the ANPE procedure demonstrates the better detection performance in comparison with the sliding window technique.

Both GD and OS-CFAR detector present good robustness when the interfering targets are presented with vantage to the GD while the detection performance degradation of the CA-CFAR detector is evident.

## 6 Acknowledgment

This research was supported by the SL Corporation and Industry-Academic Cooperation Foundation of KNU within the limits of the research project on design and development of signal detection algorithms for car applications, (grant no. 20101459000) and Kyungpook National University Grant, 2013. Additionally, the authors would like to thank the anonymous reviewers for the comments and suggestions that helped to improve a quality of the present paper.

## 7 References

1 Xu, X., Jing, Y., Yu, X.: 'Subspace-based noise variance and SNR estimation for OFDM systems'. Proc. IEEE Wireless Communications and Networking Conf., Nanjing, China, March 2005, vol. 1, pp. 23–26
2 Manzoor, R.S., Jeoti, V., Kamel, N., Asif, M.: 'A novel noise power and SNR estimation in WiMAX systems'. Proc. Int. Symp. Information Technology (ITSim 2008), Malaysia, August 2008, vol. 4, pp. 1–6
3 Manzoor, R.S., Majavu, W., Jeoti, V., Kamel, N., Asif, M.: 'Front-end estimation of noise power and SNR in OFDM systems'. Proc. Int. Conf. Intelligent and Advanced Systems (ICIAS 2007), Malaysia, November 2007, pp. 435–439
4 Mariani, A., Giorgetti, A., Chiani, M.: 'Effects of noise power estimation on energy detection for cognitive radio applications', *IEEE Trans. Commun.*, 2011, **59**, (12), pp. 3410–3420
5 Richards, M.A.: 'Fundamentals of radar signal processing' (McGraw-Hill, New York, 2005)
6 Finn, H., Johnson, R.: 'Adaptive detection mode with threshold control as a function of spatially sampled clutter-level estimates', *RCA Rev.*, 1968, **29**, (3), pp. 414–464
7 Rohling, H.: 'Radar CFAR thresholding in clutter and multiple target situations', *IEEE Trans. Aerosp. Electron. Syst.*, 1983, **19**, (4), pp. 608–621
8 Himonas, S.D., Barkat, M.: 'A robust radar CFAR detector for multiple target situations'. Proc. IEEE National Radar Conf., Dallas, USA, March 1989, pp. 85–90
9 Himonas, S.D.: 'Adaptive censor greatest-of CFAR detection', *IEE Proc. F, Radar Signal Process.*, 1992, **139**, (3), pp. 247–255
10 Gandhi, P.P., Kassam, S.A.: 'Analysis of CFAR processors in nonhomogeneous background', *IEEE Trans. Aerosp. Electron. Syst.*, 1988, **24**, (4), pp. 427–445
11 Kim, C.J., Lee, H.S.: 'Detection analysis of a generalized order statistics CFAR detector for a correlated Rayleigh target', *Signal Process.*, 1995, **47**, pp. 227–233
12 Kim, C.J.: 'A new formula to predict the exact detection probability of a generalized order statistics CFAR detector for a correlated rayleigh target', *ETRI J.*, 1994, **16**, (2), pp. 15–25
13 Kraut, S., Scharf, L.L., McWhorter, L.T.: 'Adaptive subspace detectors', *IEEE Trans. Signal Process.*, 2001, **49**, (1), pp. 1–16
14 Tuzlukov, V.: 'A new approach to signal detection theory', *Digit. Signal Process.*, 1998, **8**, (3), pp. 166–184
15 Tuzlukov, V.: 'Signal detection theory' (Springer-Verlag, Boston, 2001)
16 Tuzlukov, V.: 'Signal processing noise' (CRC Press, Taylor & Francis Group, Boca Raton, London, New York, Washington D.C., 2002)
17 Maximov, M.: 'Joint correlation of fluctuative noise at outputs of frequency filters', *Radio Eng.*, 1956, **9**, pp. 28–38
18 Chernyak, Y.: 'Joint correlation of noise voltage at outputs of amplifiers with nonoverlapping responses', *Radio Phys. Electron.*, 1960, **4**, pp. 551–561
19 Tuzlukov, V.: 'Generalized approach to signal processing in wireless communications: the main aspects and some examples', in: 'Wireless communications and networks – recent advances' ed: Eksim, A. (In Tech, Rijeka, Croatia, 2012), Ch. 11, pp. 305–338
20 Tuzlukov, V.: 'DS-CDMA downlink systems with fading channel employing the generalized receiver', *Digit. Signal Process.*, 2011, **21**, pp. 725–733
21 Tuzlukov, V.: 'Signal processing by generalized receiver in DS-CDMA wireless communication systems with frequency-selective channels', *Circuits Syst. Signal Process.*, 2011, **30**, pp. 1197–1230
22 Tuzlukov, V.: 'Signal processing by generalized receiver in DS-CDMA wireless communication systems with optimal combining and partial cancellation', *EURASIP J. Adv. Signal Process.*, 2011, pp. 1–15, Article ID 913189, doi:10.1155/2011/913189
23 Tuzlukov, V.: 'Signal processing in radar systems' (CRC Press, Taylor & Francis Group, Boca Raton, London, New York, Washington D.C., 2012)
24 Shbat, M.S., Tuzlukov, V.: 'Noise power estimation under generalized detector employment in automotive detection and tracking systems'. Proc. Ninth IET Data Fusion and Target Tracking Conf. (DF&TT'12), London, UK, May 2012, doi: 10.1049/cp.2012.0416
25 Shbat, M.S., Tuzlukov, V.: 'Generalized approach to signal processing in noise for closing vehicle detection application using FMCW radar sensor system'. Proc. Int. Radar Symp. (IRS 2011), Leipzig, Germany, September 2011, pp. 459–464
26 Shbat, M.S., Tuzlukov, V.: 'Signal processing in automotive controller area network based on radar sensors'. Proc. 11th Int. Conf. Control, Automation, and Systems (ICCAS 2011), Gyeonggi-do, South Korea, October 2011, pp. 616–620




doi: 10.1049/iet-spr.2013.0235

27 Shbat, M.S., Tuzlukov, V.: 'Generalized detector with adaptive detection threshold for radar sensors'. Proc. Int. Radar Symp. (IRS 2012), Warsaw, Poland, May 2012, pp. 91–94
28 Yeh, C., Robel, A.: 'Adaptive noise level estimation'. Proc. Ninth Int. Conf. Digital Audio Effects (DAFx-06), Montreal, Canada, September 2006, pp. 145–148
29 Bertsekas, D.P.: 'Constrained optimization and lagrange multiplier methods' (Athena Scientific, Belmont, MA, USA, 1996)
30 Rohling, H.: 'Some radar topics: waveform design, range CFAR and target recognition', *Adv. Sens. Sec. Appl. NATO Sec. Sci. Ser.*, 2006, **2**, pp. 293–322
31 Gandhi, P., Kassam, S.: 'Analysis of CFAR processors in nonhomogeneous background', *IEEE Trans. Aerosp. Electron. Syst.*, 1988, **24**, (4), pp. 427–445
32 Khalighi, M.A., Bastani, M.H.: 'Adaptive CFAR processor for nonhomogeneous environments', *IEEE Trans. Aerosp. Electron. Syst.*, 2000, **36**, (3), pp. 889–897
33 Magaz, B., Belouchrani, A., Hamadouche, M.: 'Automatic threshold selection in OS-CFAR radar detection using information theoretic criteria', *Prog. Electromagn. Res. B*, 2011, **30**, pp. 157–175
34 Kay, S.: 'Fundamentals for statistical signal processing, vol. 1: estimation theory' (Prentice-Hall, Englewood Cliffs, NJ, 1993)
35 Gradshteyn, I., Ryzhik, I.: 'Table of integrals, series, and products' (Academic Press, New York, 1994, 5th edn.)
36 Kay, S.: 'Fundamentals for statistical signal processing, vol. 2: detection theory' (Prentice-Hall PTR, NJ, 1998)
37 Mahafza, B.R., Elsherbeni, A.Z.: 'Matlab simulation for radar systems design' (Chapman & Hall/CRC Press LLC, 2004)